

## **CHAPTER 4**

# **Characterization of Material**

## CHAPTER 4

### Characterization of Material

Quantum dots of metal oxide semiconductors exhibit many interesting electronic, optoelectronic and optical properties <sup>[1-29]</sup>. These properties become more interesting when the size of the quantum dots becomes very small (less than 1000 nm). To explore these properties of our synthesized metal oxide semiconductors quantum dots, the following characterizations have been carried out, which is my contribution to this chapter.

- (i) UV-Visible Spectroscopy
- (ii) X-ray diffraction study (XRD)
- (iii) High Resolution Transmission Electron Microscopy (HRTEM)

In this chapter, the characterizations of the samples by the above mentioned techniques have been explained. The average crystallite size of the quantum dots is estimated by XRD, and HRTEM studies. The variation of band gap that occurs due to variation of size of the quantum dots has been explored by optical absorption spectroscopy.

#### 4.1. UV- Visible spectroscopy

Ultraviolet-visible (UV-VIS) spectroscopy involves the spectroscopy of photons in the UV-visible region. It uses light in the visible and adjacent near ultraviolet (UV) and near infrared (NIR) ranges. In this region of the electromagnetic spectrum,

molecules undergo electronic transitions. This technique is complementary to fluorescence spectroscopy. Fluorescence deals with transitions from the excited state to the ground state, while absorption measures transitions from the ground state to the excited state.

The instrument used in ultraviolet-visible spectroscopy is called a UV-VIS spectrophotometer. It measures the intensity ( $I$ ) of light passing through a sample and compares it to the intensity ( $I_0$ ) of light before it passes through the sample. The ratio  $I / I_0$  is called the transmittance, and is usually expressed as a percentage (%T). The absorbance,  $A$ , is based on the transmittance as

$$A = -\log (\%T) \dots\dots\dots (4.1)$$

Optical absorbance ( $A$ ) is an important way to explore the different energy states in semiconductor material. This study <sup>[10-12]</sup> is based on the fact that, if two possible energy states  $E_1$  and  $E_2$  exist in a system as shown in Figure 4.1, then electronic transition from level  $E_1$  to  $E_2$  can take place when appropriate energy  $E_2 - E_1 = \Delta E$  is absorbed and the frequency of radiation has the simple form of

$$\nu = \frac{\Delta E}{h} \text{ Hz}$$

$$\text{or, } \Delta E = h\nu \text{ joules.} \dots\dots\dots(4.2)$$

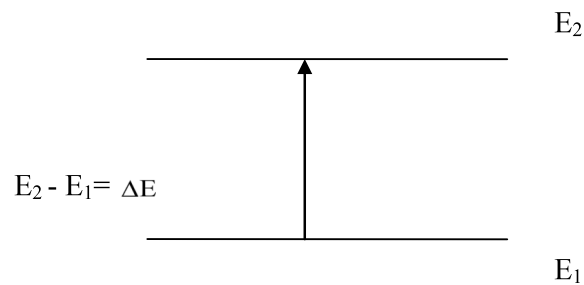


**Fig.4.1. Schematic diagram of Electronic excitation between two energy states**

That is, absorption wavelength or edge can be written as

$$\lambda_a = \frac{hc}{\Delta E} \dots\dots\dots(4.3)$$

Where ‘ $\lambda_a$ ’ is the absorption edge, ‘ $h$ ’ is the Planck’s constant and ‘ $c$ ’ is the velocity of light.

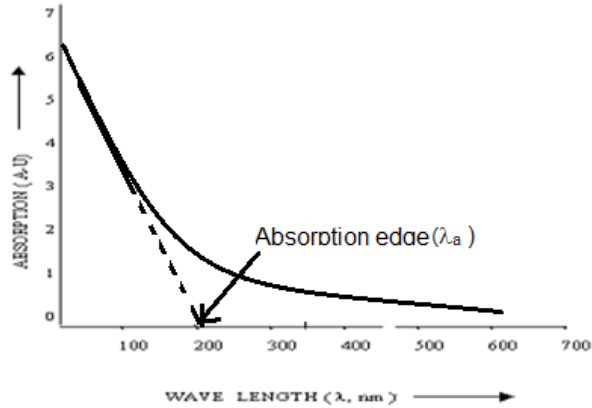


**Fig. 4.2. Schematic of UV / Visible absorption spectra**

**4.2 X-ray diffraction study (XRD)**

X-ray diffraction study is an important tool for finding different crystal parameters like crystallite size, d-spacing, diffraction planes, structure, phase, and lattice constants, etc. The intensities and the angles of diffracted X-ray beams are related to atomic arrangement of the crystal.

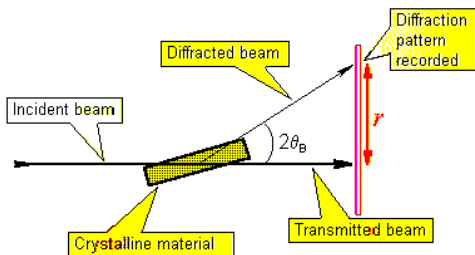


**Fig.4.3. X-ray diffraction by sample.**



**Fig.4.4. A typical X-ray diffractometer.**

In this study, X-ray diffractometer detects the X-ray, diffracted by crystal and gives the diffractogram, which is a plot between intensity and diffraction angle. Intensity is given in terms of arbitrary units (A.U) and the angle is in degrees. Figure 4.5 shows a schematic of pattern of such X-ray diffractogram.

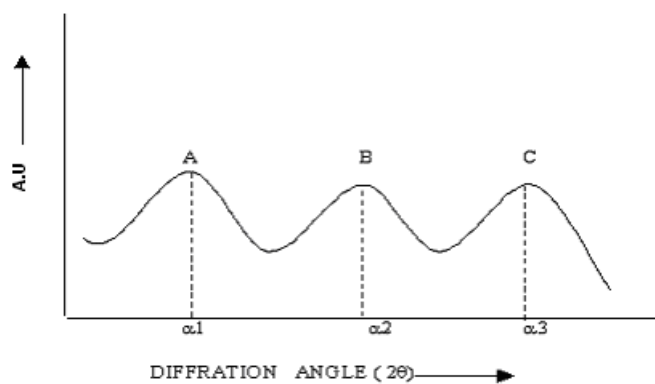


**Fig 4.5. Schematic of XRD pattern.**

Next we explain how X-ray diffractogram is used in finding various crystal parameters of the quantum dots, prepared in our laboratory.

#### **4.2.1. Sample identification**

To identify any specimen, the diffraction angles produced by a particular sample are compared with the standard diffraction angles of the same material. A good match between experimental and standard values of diffraction angles is required to identify the specimen. The most commonly used database for the identification of crystal structures is ICDD (International Center Diffraction Data) system.

**4.2.2. Crystallite (grain) size estimations**

A crystallite is a single crystal in a polycrystalline aggregate. X-ray diffractogram is extensively used to calculate the average crystallite size (D) using Debye-Scherrer equation [9]. The equation is written as

$$D = \frac{0.9\lambda}{W \cos\theta} \dots\dots\dots(4.4)$$

Where  $\lambda$  is the wavelength of X-ray used, W is the corrected full width at half maximum (FWHM) for instrumental broadening,  $\theta$  is the glancing angle in radians. The different parameters used in equation (4.4) can be obtained from X-ray diffractogram, in the following way

**I. Full Width at Half Maximum (FWHM)**

In the example shown in Figure 4.6, the maximum height of the XRD peak is BC and OB is the noise. Half of the maximum height is either AB or AC. That is, the middle point of the peak is A. Two more points P and Q are taken on the plot collinear to point A. Two perpendiculars from points P and Q are drawn on the abscissa, which is cut by the perpendicular lines at point R and S. The segment RS is the full width at half maximum (FWHM) in degrees. Finally, this is converted into radians, which is the required FWHM (W).

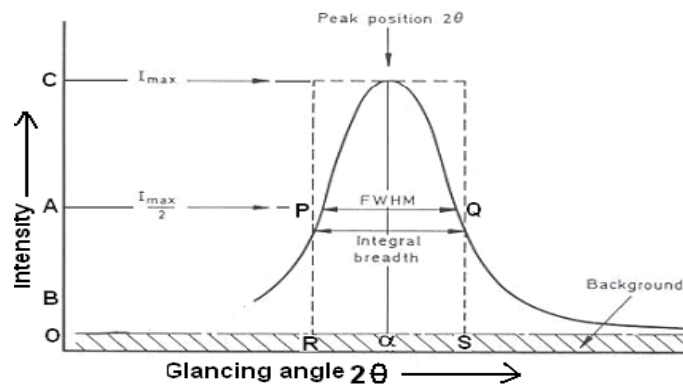


**Fig.4.6. Schematic of Single XRD peak.**

## **II. Diffraction angle or glancing angle ( $\theta$ ) and X-ray wavelength**

In the diffractogram, the angle axis is calibrated in terms of “ $2\theta$  / degree”. From this, glancing angle “ $\theta$ ” can be obtained. The X-ray wavelength “ $\lambda$ ” used in the X-ray diffractometer is 1.541 Angstrom.

In practice, the experimental data obtained from XRD study of any specific specimen may slightly differ from the standard values due to the following reasons.

1. Calibration error
2. Instrumental error
3. Sudden power fluctuation during experiment
4. External noises.

The X-ray diffraction (XRD) analyses of quantum dot samples are carried out using a PAN analytical X’Pert Pro X-ray Diffractometer with Cu  $K_{\alpha}$  radiation as an X-ray source at 40 kV and 30 mA in a scanning angle ( $2\theta$ ) ranging from  $20^{\circ}$  to  $70^{\circ}$  with scan speed  $0.001^{\circ}\text{s}^{-1}$ . Various XRD data have been calculated using X’Pert High Score software.

Using ICDD (International Center Diffraction Data) sample parameters (Size, lattice constants, crystal planes etc.) are obtained very easily now a days.

### **4.3 High Resolution Transmission Electron Microscopy (HRTEM):**

HRTEM has opened a new door to nano-science research by providing pictorial view of them with very high magnification of 8 lacks or more. This study, gives the information about size, shape and surface morphology of any specimen. High

Resolution Transmission electron microscopy (HRTEM) is a microscopy technique whereby a beam of electrons is transmitted through the specimen. An image is formed from the electrons, transmitted through the specimen which is magnified and focused by an objective lens and appears on an imaging screen, a fluorescent screen is used in most HRTEMs, and also the image is recorded by a sensor such as a CCD camera.



**Fig.4.7. Photographs of high resolution transmission electron microscope.**

#### **4.4. Conductivity Test**

To test the conductivity of the samples, whether p-type or n-type, a simple method called ‘thermoelectric effect’ have been used <sup>[16]</sup>. A measurement of the sign of the voltage across a semiconductor specimen, one end of which is heated is a rough and ready way to tell if the specimen is n-type or p-type. For p-type semiconductor, the sign is positive (+ve), and negative (-ve) for n-type semiconductor. In this work, the conductivity of all the prepared samples (ZnO, SnO<sub>2</sub> and Fe<sub>2</sub>O<sub>3</sub>) are tested by the



method and are found to possess n-type conductivity. The results are verified by “Hall effect” also.

#### 4.5. Characterization of samples

In the next consecutive sections, the characterizations of our prepared semiconductor metal oxide quantum dots are discussed in details.

##### 4.5.1. Zinc oxide (ZnO) quantum dots embedded in PVA (Polyvinyl Alcohol) matrix

ZnO specimen <sup>[29]</sup> has been characterized by UV/VIS optical absorption spectroscopy (Perkin Elmer Lamda 35 1.24), X-ray diffraction study (Bruker AXS, X-ray source: Cu K<sub>α</sub>) and high resolution transmission electron microscopy (HRTEM) (JEM 2100, Jeol).

##### I. Optical absorption spectroscopy

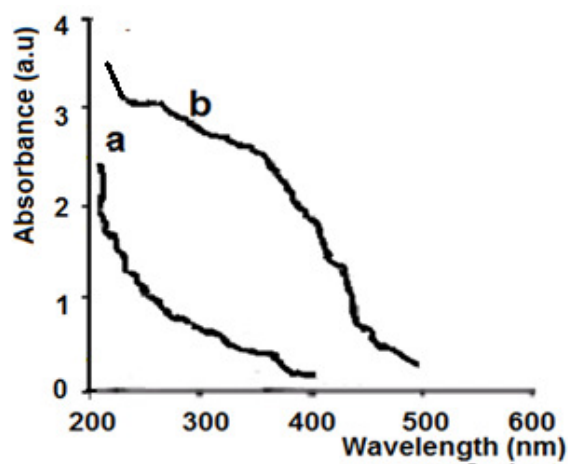


Fig. 4.8. Optical spectra of ZnO a: quantum dot, b: bulk

In the optical absorbance spectra shown in Figure 4.8, “a” denotes the spectrum of ZnO quantum dot while “b” denotes that of bulk. It is seen that the band edge absorption in quantum dot is strongly blue shifted at 215 nm with respect to bulk specimen which possesses the absorption edge at around 390 nm. For estimating particle size from blue shift, a theoretical model <sup>[7,8]</sup> has been proposed, known as hyperbolic band model that is written as

$$R = \sqrt{\frac{2\pi^2 h^2 E_{gb}}{m^* (E_{gn}^2 - E_{gb}^2)}} \dots\dots\dots (4.5)$$

Where, R is the quantum dot radius,  $E_{gb}$  is the bulk band gap,  $E_{gn}$  is the quantum dot band gap, h is Planck’s constant,  $m^*$  is the effective mass of the specimen. The bulk band gaps at room temperature and the effective mass <sup>[6,7]</sup> of ZnO is listed in the Table 4.1.

Name of the samples	Bulk Band gap	Values of effective mass	Structure
ZnO	3.20 eV	$2.45 \times 10^{-31}$ Kg	wurzite

**Table 4.1. Bulk band gap and effective masses of ZnO**

The data obtained from the analysis are put in Table 4.2.

Absorption edge in quantum dot	Energy gap in quantum dot	Bulk absorption edge	Bulk band gap	Enhancement in band gap due to size quantization	Quantum dot size
215 nm	5.2 eV	390 nm	3.20 eV	2 eV	12 nm

**Table.4.2. Data of ZnO/PVA specimen revealed from optical absorption spectroscopy.**

## II. X-ray diffraction study

From X-ray diffraction study (Figure 4.9) average particle size (crystallite size) is calculated by using Debye-Scherrer formula<sup>[9]</sup>  $D = \frac{0.9\lambda}{W \cos\theta}$ , ‘ $\lambda$ ’ is wave length of X-ray (0.1541 nm), ‘W’ is FWHM (full width at half maxima), ‘ $\theta$ ’ (theta) is the glancing angle and ‘D’ is particle diameter (crystallite size). Considering all the peaks<sup>[2]</sup> ( $2\theta$  in degree) in the X-ray diffractogram, the average crystallite (quantum dot) size has been assessed and found to be 11 nm. Further, by analyzing the X-ray diffractogram with the help of ICDD (International Center Diffraction Data) it has been revealed that ZnO quantum dots are wurzite in structure.

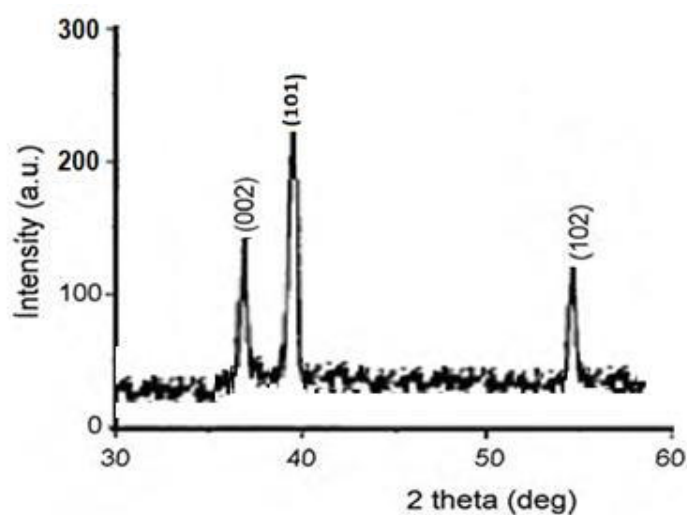
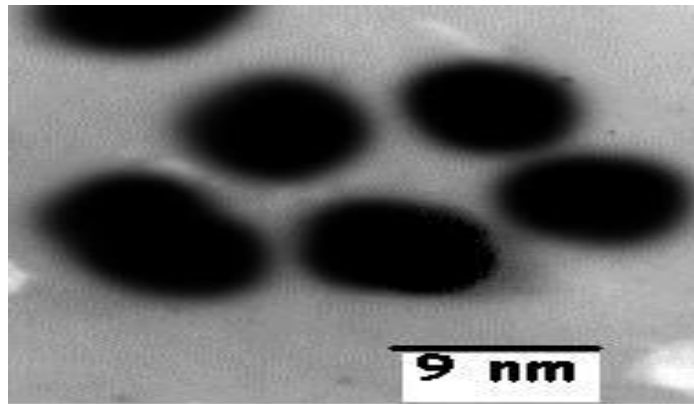


Fig 4.9: XRD Spectra of ZnO Quantum dots embedded in PVA

## III. High Resolution Transmission Electron Microscopy (HRTEM)

HRTEM photograph of ZnO quantum dots<sup>[29]</sup> is shown in Figure 4.10 which provides the surface morphological view of the particles. The sample size and shapes are put in the Table 4.3.



**Fig.4.10. HRTEM Photographs of ZnO**

Average particle size	Particle Shape
11 nm	Elliptical

**Table. 4.3. Data of ZnO/PVA sample obtained from HRTEM study**

All these characterizations infer that sizes of ZnO quantum dots are within 12 nm.

#### **4.5.2 Zinc oxide (ZnO) quantum dots embedded in PVP (Polyvinyl Pyrrolidone) matrix**

ZnO specimen<sup>[28]</sup> has been characterized by UV/VIS optical absorption spectroscopy (Perkin Elmer Lamda 35 1.24), X-ray diffraction study (Bruker AXS, X-ray source: Cu K $\alpha$ ) and high resolution transmission electron microscopy (HRTEM) (JEM 2100, Jeol).

## II. Optical absorption spectroscopy

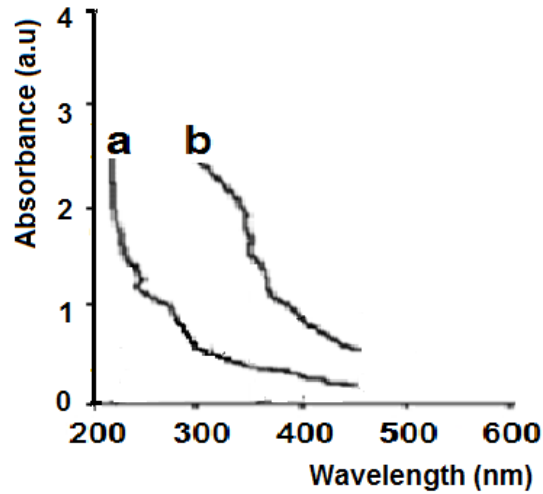


**Fig. 4.11. Optical spectra of ZnO embedded on PVP a: quantum dot, b: bulk**

In the optical absorbance spectra shown in Figure 4.11, “a” denotes the spectrum of ZnO quantum dot<sup>[28]</sup> while “b” denotes that of bulk. It is seen that the band edge absorption in quantum dot is strongly blue shifted at 210 nm with respect to bulk specimen which possesses the absorption edge at around 390 nm. For estimating particle size from blue shift, a theoretical mode<sup>[7,8]</sup> has been proposed, known as hyperbolic band model that is written as

$$R = \sqrt{\frac{2\pi^2 h^2 E_{gb}}{m^* (E_{gn}^2 - E_{gb}^2)}} \dots\dots\dots (4.6)$$

Where, R is the quantum dot radius,  $E_{gb}$  is the bulk band gap,  $E_{gn}$  is the quantum dot band gap, h is planck’s constant,  $m^*$  is the effective mass of the specimen. The bulk band gaps at room temperature and the effective mass<sup>[6,7]</sup> of ZnO is listed in the Table 4.4.

Name of the samples	Bulk Band gap	Values of effective mass	Structure
ZnO	3.20 eV	$2.45 \times 10^{-31}$ Kg	wurzite

**Table 4.4. Bulk band gap and effective masses of ZnO**

The data obtained from the analysis are put in Table 4.5.

Absorption edge in quantum dot	Energy gap in quantum dot	Bulk absorption edge	Bulk band gap	Enhancement in band gap due to size quantization	Quantum dot size
210 nm	5.3 eV	390 nm	3.20 eV	2.10 eV	10 nm

**Table.4.5. Data of ZnO/PVP specimen revealed from optical absorption spectroscopy.**

## II. X-ray diffraction study

From X-ray diffraction study (Figure 4.12) average particle size (crystallite size) is

calculated by using Debye-Scherrer formula<sup>[9]</sup>  $D = \frac{0.9\lambda}{W \cos\theta}$ , ‘ $\lambda$ ’ is wave length of

X-ray (0.1541 nm), ‘W’ is FWHM (full width at half maxima), ‘ $\theta$ ’ (theta) is the glancing angle and ‘D’ is particle diameter (crystallite size). Considering all the peaks<sup>[2]</sup> ( $2\theta$  in degree) in the X-ray diffractogram, the average crystallite (quantum dot) size has been assessed and found to be 9 nm. Further, by analyzing the X-ray diffractogram with the help of ICDD (International Center Diffraction Data) it has been revealed that ZnO quantum dots are “wurzite” in structure.

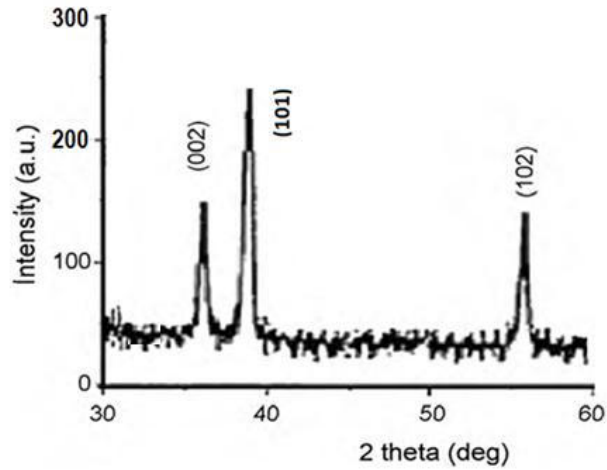


**Fig 4.12: XRD Spectra of ZnO embedded in PVP**

### **III. High Resolution Transmission Electron Microscopy (HRTEM):**

HRTEM images of PVP film (4.13.i.a) and ZnO quantum dots (4.13.i.b) are shown in Figure 4.13. It is evident in the HRTEM image (4.13.i.b) that ZnO crystallites (quantum dots) are circular in shape with sizes within 10 nm. Fig (4.13.ii) shows the Scanning Electron Microscope (SEM) image of ZnO quantum dot surface<sup>[28]</sup>. ZnO sample sizes assessed from these three studies are well matching, which is a distinct advantage over earlier reports<sup>[2,3]</sup>. All these characterizations infer that sizes of ZnO quantum dots (diameter) are within 10 nm.

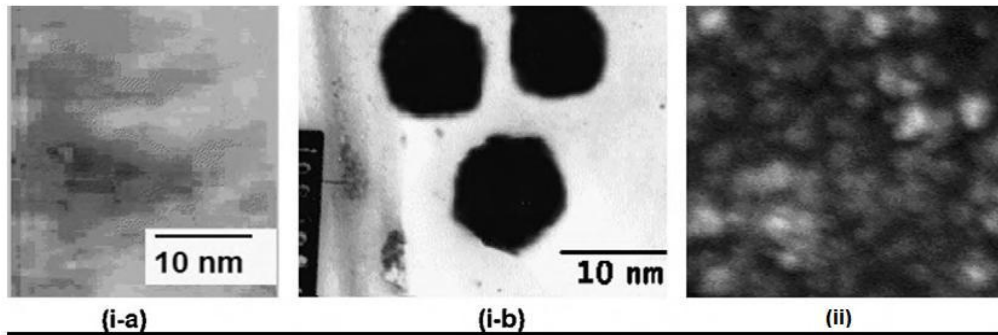


**Fig4.13: (i-a) HRTEM images of PVP matrix. (i-b) ZnO quantum dots embedded in PVP. (ii) Image Of ZnO quantum dot surface**

### 4.5.3 Tin oxide (SnO<sub>2</sub>) quantum dots embedded in PVP matrix

SnO<sub>2</sub> specimen<sup>[22]</sup> has been characterized by UV/VIS optical absorption spectroscopy (Perkin Elmer Lambda 35 1.24), X-ray diffraction study (Bruker AXS, X-ray source: Cu K<sub>α</sub>) and high resolution transmission electron microscopy (HRTEM) (JEM 2100, Jeol).

#### I. Optical absorption spectroscopy

In the optical absorbance spectra shown in Figure 4.14, denotes the spectrum of SnO<sub>2</sub> quantum dot (prepared sample)<sup>[22]</sup>. It is seen that the band edge absorption in quantum dot is strongly blue shifted at 230 nm with respect to bulk specimen which possesses the absorption edge at around 340 nm. Blue shift is a distinct signature of quantum dot formation<sup>[1,2,4]</sup>. For estimating particle size from blue shift, a theoretical model<sup>[6,7]</sup> has been proposed, known as hyperbolic band model<sup>[5]</sup> that is written as

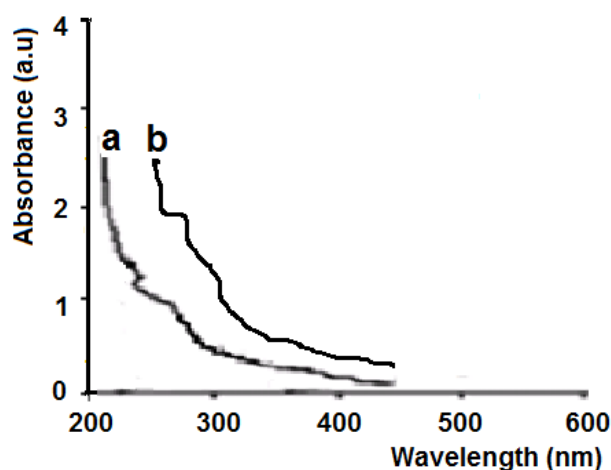


**Fig. 4.14: UV/VIS absorption spectra of SnO<sub>2</sub> a. quantum dots embedded on PVP**



$$R = \sqrt{\frac{2\pi^2 \hbar^2 E_{gb}}{m^* (E_{gn}^2 - E_{gb}^2)}} \dots\dots\dots(4.7)$$

Where, R is the quantum dot radius,  $E_{gb}$  is the bulk band gap,  $E_{gn}$  is the quantum dot band gap,  $\hbar$  is planck's constant,  $m^*$  is the effective mass of the specimen. The bulk band gaps at room temperature and the effective mass<sup>[6,7]</sup> of  $\text{SnO}_2$  is listed in the Table 4.6.

Name of the samples	Bulk Band gap	Values of effective mass ( $m^*$ )	Structure
$\text{SnO}_2$	3.6 eV	$2.51 \times 10^{-31}$ Kg	Rutile structure

**Table 4.6. Bulk band gap and effective masses of  $\text{SnO}_2$**

The data obtained from the analysis are put in Table 4.7.

Absorption edge in quantum dot	Energy gap in quantum dot	Bulk absorption edge	Bulk band gap	Enhancement in band gap due to size quantization	Quantum dot size
230 nm	4.4 eV	340 nm	3.6 eV	0.8 eV	13 nm

**Table.4.7. Data of  $\text{SnO}_2$ /PVP specimen revealed from optical absorption spectroscopy**

## II. X-ray diffraction study

From X-ray diffraction study (Figure 4.15) average particle size (crystallite size) is

calculated by using Debye-Scherrer formula<sup>[9]</sup>  $D = \frac{0.9\lambda}{W \cos\theta}$ , ' $\lambda$ ' is wave length of

X-ray (0.1541 nm), ' $W$ ' is FWHM (full width at half maxima), ' $\theta$ ' (theta) is the glancing angle and ' $D$ ' is particle diameter (crystallite size). Considering all the

peaks<sup>[2]</sup> ( $2\theta$  in degree) in the X-ray diffractogram, the average crystallite (quantum dot) size has been assessed and found to be 12 nm. Further, by analyzing the X-ray diffractogram with the help of ICDD (International Center Diffraction Data) it has been revealed that  $\text{SnO}_2$  quantum dots are rutile in structure.

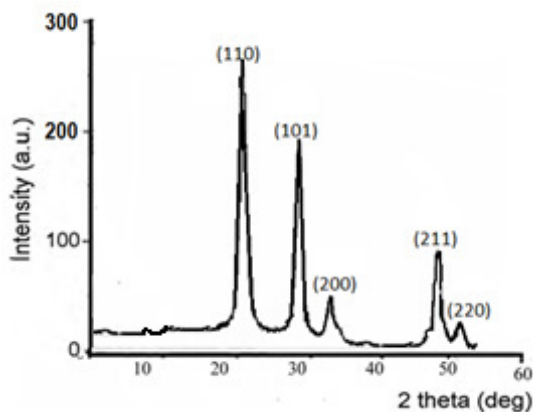


**Fig. 4.15: XRD spectra of  $\text{SnO}_2$  quantum dots**

### III. High Resolution Transmission Electron Microscopy (HRTEM)

HRTEM images of PVP film (4.16.c) and  $\text{SnO}_2$  quantum dots (4.16.a,b) are shown in Figure 4.16. It is evident in the HRTEM image (4.16.a) that  $\text{SnO}_2$  crystallites (quantum dots) are circular in shape with sizes within 12 nm<sup>[22]</sup>.

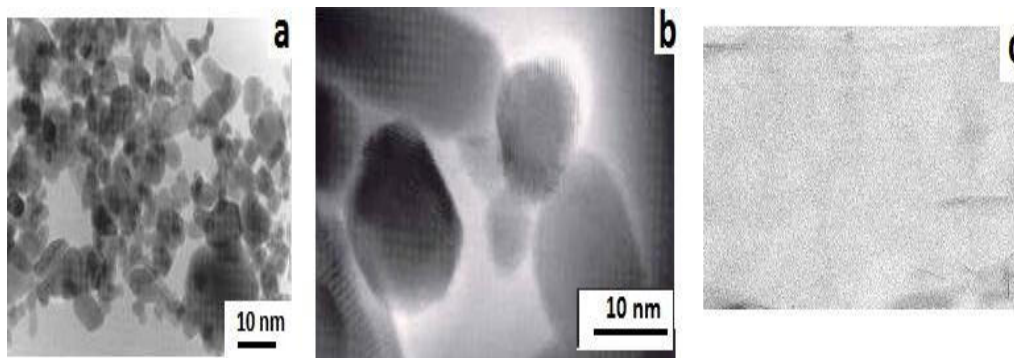


**Fig. 4.16: HRTEM images of  $\text{SnO}_2$  sample**

SnO<sub>2</sub> sample sizes assessed from these three studies are well matching. This matching occurs due to the formation of well uniformed and circular shaped quantum dots by using PVP matrix<sup>21</sup>. All these characterizations infer that average size of SnO<sub>2</sub> quantum dots (diameter) are within 13 nm.

#### 4.5.4 Iron oxide (Fe<sub>2</sub>O<sub>3</sub>) quantum dots embedded in PVP matrix

Fe<sub>2</sub>O<sub>3</sub> specimen<sup>[23]</sup> has been characterized by UV/VIS optical absorption spectroscopy (Perkin Elmer Lamda 35 1.24), X-ray diffraction study (Bruker AXS, X-ray source: Cu K<sub>α</sub>) and high resolution transmission electron microscopy (HRTEM) (JEM 2100, Jeol).

##### I. Optical absorption spectroscopy

In the optical absorbance spectra shown in Figure 4.17, denotes the spectrum of Fe<sub>2</sub>O<sub>3</sub> quantum dot (prepared sample)<sup>[23]</sup>. It is seen that the band edge absorption in quantum dot is strongly blue shifted at 290 nm with respect to bulk specimen which possesses the absorption edge at around 650 nm.. For estimating particle size from blue shift, a theoretical model<sup>[6,7]</sup> has been proposed, known as hyperbolic band model that is written as

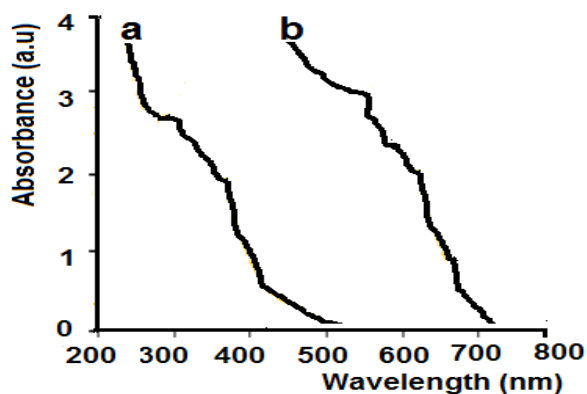


Fig. 4.17: UV/VIS absorption spectra of Fe<sub>2</sub>O<sub>3</sub> a. quantum dots embeddedon PVP b. bulk

$$R = \sqrt{\frac{2\pi^2 h^2 E_{gb}}{m^*(E_{gn}^2 - E_{gb}^2)}} \dots\dots\dots(4.8)$$

Where, R is the quantum dot radius, E<sub>gb</sub> is the bulk band gap, E<sub>gn</sub> is the quantum dot band gap, h is planck’s constant, m\* is the effective mass of the specimen. The bulk band gaps at room temperature and the effective mass<sup>[6,7]</sup> of Fe<sub>2</sub>O<sub>3</sub> is listed in the Table 4.8.

Name of the samples	Bulk Band gap	Values of effective mass	Structure
Fe <sub>2</sub> O <sub>3</sub>	2.2 eV	2.49 x 10 <sup>-31</sup> Kg	wurzite

**Table 4.8. Bulk band gap and effective masses of Fe<sub>2</sub>O<sub>3</sub>**

The data obtained from the analysis are put in Table 4.9.

Absorption edge in quantum dot	Energy gap in quantum dot	Bulk absorption edge	Bulk band gap	Enhancement in band gap due to size quantization	Quantum dot size
290 nm	3.4 eV	650 nm	2.2 eV	1.2 eV	15 nm

**Table.4.9. Data of Fe<sub>2</sub>O<sub>3</sub>/PVP specimen revealed from optical absorption spectroscopy**

## II. X-ray diffraction study

From X-ray diffraction study (Figure 4.18) average particle size (crystallite size) is calculated by using Debye-Scherrer formula<sup>[9]</sup>  $D = \frac{0.9\lambda}{W \cos\theta}$ , ‘λ’ is wave length of X-ray (0.1541 nm), ‘W’ is FWHM (full width at half maxima), ‘θ’ (theta) is the glancing angle and ‘D’ is particle diameter (crystallite size). Considering all the

peaks<sup>[3]</sup> ( $2\theta$  in degree) in the X-ray diffractogram, the average crystallite (quantum dot) size has been assessed and found to be 14 nm. Further, by analyzing the X-ray diffractogram with the help of ICDD (International Center Diffraction Data) it has been revealed that  $\text{Fe}_2\text{O}_3$  quantum dots are “wurzite” in structure.

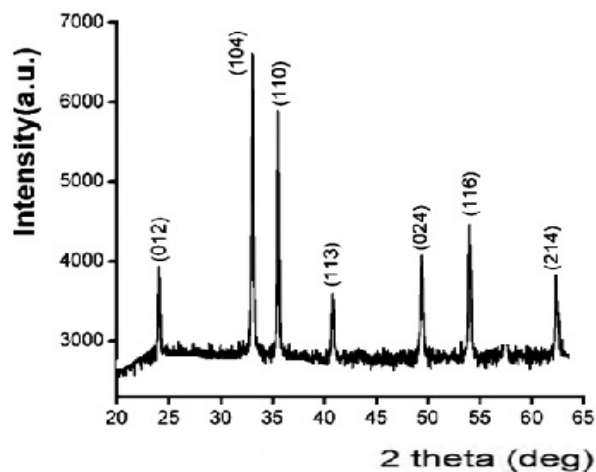


**Fig. 4.18: XRD spectra of  $\text{Fe}_2\text{O}_3$  quantum dots**

### III. High Resolution Transmission Electron Microscopy (HRTEM)

HRTEM images of Plane-view(4.19.a) and cross sectional view of (4.19.b) of  $\text{Fe}_2\text{O}_3$  quantum dots are shown in Figure 4.19. It is evident in the HRTEM image (4.19.a) that  $\text{Fe}_2\text{O}_3$  crystallites (quantum dots) are circular in shape with sizes within 15 nm.

[23]

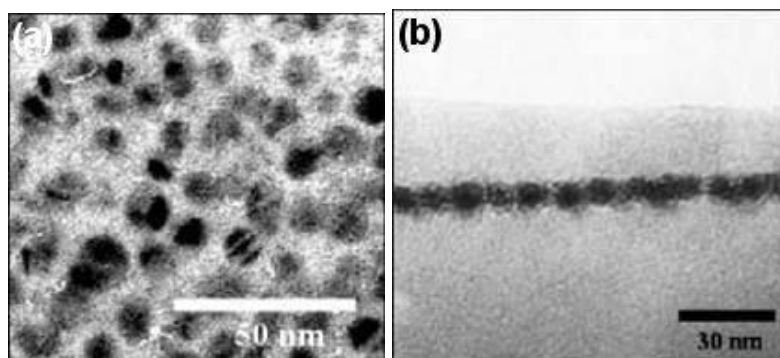


**Fig. 4.19: HRTEM images of  $\text{Fe}_2\text{O}_3$  sample**

Fe<sub>2</sub>O<sub>3</sub> sample sizes <sup>[23]</sup> assessed from these three studies are well matching. This matching occurs due to the formation of well uniformed and circular shaped quantum dots by using PVP matrix instead of PVA (polyvinyl alcohol) matrix<sup>[2]</sup>. All these characterizations infer that sizes of Fe<sub>2</sub>O<sub>3</sub> quantum dots (diameter) are within 15 nm.

**4.6 Conclusion:** The prepared quantum dots have been characterized by various techniques, namely UV/VIS spectrometry, XRD and HRTEM. The characterizations infer that ZnO quantum dots are within 12 nm and 10 nm on PVA and PVP respectively. Further, it has been inferred that ZnO quantum dots are uniformly arranged on PVP rather than on PVA. In case of SnO<sub>2</sub> quantum dots, the size is within 13 nm while the size of Fe<sub>2</sub>O<sub>3</sub> is within 15 nm. the structures of ZnO, Fe<sub>2</sub>O<sub>3</sub> the quantum dots are wurtzite while the structure of SnO<sub>2</sub> is rutile.

#### **References:**

- [1] Zhang, K.; Chang, H.Y.; Fu, A.H.; Alivisatos, A.P. and Yang, H., Continuous distribution of emission states from single CdSe/ZnS quantum dots, *Nano Lett.*, vol. 6, pp.843–847, 2006.
- [2] Nath, S.S.; Chakdar, D.; Gope,G. and Avasthi, D.K., Effect of 100 MeV Nickel Ions on Silica Coated ZnS quantum Dots, *J. Nanoelectronics and Optoelectronics.*, vol. 3, No. 2,pp. 180-183, 2008.

- [3] Nath, S.S.; Chakdar, D; Gope,G. and Avasthi, D.K., Novel effect of swift heavy ion on ZnO quantum dots prepared by quenching method, *Nanotrends J. nanotech. its application*, vol.3, pp.1-10, 2008.
- [4] Nath, S.S.; Chakdar, D.; Gope,G.; Kakati, J.; Kalita,B.; Talukdar, A. and Avasthi, D.K., Green luminescence of ZnS and ZnS:Cu quantum dots embedded in zeolite matrix, *J. Appl. Phys.*, vol.105, pp.094305–94309,2009.
- [5] Nanda, J.J. and Sarma, D.D., Photoemission spectroscopy of size selected zinc sulfide nanocrystallites, *J Appl. Phys.*,vol. 90 , pp.2504–2511, 2001.
- [6] Mohanta, D.; Nath, S.S.; Bordoloi, A.; Mishra, N.C.; Dolui, S.K. and Choudhury, A., Optical absorption study of 100-MeV chlorine ion irradiated hydroxyl free ZnO semiconductor quantum dots, *J. Appl. Phys.*, vol. 92, pp.7149-7152,2002.
- [7] Nath, S.S.; Chakdar, D. and Gope, G., *Azojonano-Journal of Nanotechnology* online, vol.4, p.1, 2008.
- [8] Fallah, H.R.; Ghasemi, M.; Hassanzadeh, Ali and Steki, H., The effect of deposition rate on electrical, optical and structural properties of tin-doped indium oxide (ITO) films on glass at low substrate temperature, *Physica B.*, vol.373,pp. 274-279, 2006.
- [9] Klug, H.P. and Alexander, L.E., *X-Ray Diffraction Procedures for Polycrystalline and Amorphous Materials*, Wiley, NewYork, 1974.
- [10] Zhang, Y. C.; Huang, C. J. ; Liu, . F. Q .; Xu,B.; Wu , J.; Chen , Y.H.; Ding, D.; Jiang, W. H.; Ye, X. L. and Wang, Z. G., *J. Appl. Phys.* vol. 90, No. 4, pp 1973, 2001.

- [11] Mahamuni, S.; Bendre, B. S.; Leppert, V.J.; Smith, C. A.; Cooke, D.; Risbud, S. H. and Lee, H. W. H., *Nano. Struct. Mater.*, vol. 7, No. 6, p. 659, 1996.
- [12] Mohanta, D.; Nath, S.S.; Mishara, N.C. and Choudhury, A., *Bull. Mater. Sci.*, vol. 26, No. 3, 2003.
- [13] Adachi, A.; Kudo, A. and Sakata, T., *Bull. Chem. Soc. Jpn.*, vol.68, p. 3283, 1995.
- [14] Pankove, J.I., *Optical processes in Semiconductors*, *Dover Publications, Inc.*, *New York*, Chapter 3, p.34, 1971.
- [15] Tyagi, P. and Vedeshwar, A.G., *Bull. Mater. Sci.*, vol. 24, No. 3, pp. 297-3, June 2001.
- [16] Kittel, Charles., *Introduction to Solid State Physics*, *John Wiley & Sons*, *New York*, p.228, 1996.
- [17] Singhal, R.L., *Solid State Physics*, *Kedar Nath Ram Nath & Co*, *Meerut, U.P., India*, 1995.
- [18] Behera, S. N.; Sahu, S. N. and Nanda, K. K.; *Ind. J. Phys*, vol. 74, No.A(2), p.81, 2000.
- [19] Chen, Wei.; Wang, Zhanguo; Lin, Zhaojun and Lin, lanying, *J. Appl. Phys.*, vol.82, No. 6, p. 3111, 1997.
- [20] Mohammadikish, Maryam, Hydrothermal synthesis, characterization and optical properties of ellipsoid shape  $\alpha$ -Fe<sub>2</sub>O<sub>3</sub> nanocrystals, *Ceramics International*, vol.40, pp.1351–1358, 2014.



- [21] Culty, B.D., *Elements of X-ray Diffraction*, Addison-Wesley, New York, 1978.
- [22] Choudhury, M.; Nath, S.S. and Bhattacharjee, R., Ethanol sensing property of SnO<sub>2</sub> quantum dots embedded on PVP, *Journal of Nanotech. Prog INT.*, vol 5, Issue1, 2014.
- [23] Choudhury, M.; Nath, S.S. and Bhattacharjee, R., Methanol sensing property of Fe<sub>2</sub>O<sub>3</sub> quantum dots embedded on PVP, *International Journal of Nanoscience and Nanotechnology*, vol 5, Number 1, pp. 101-108, 2014.
- [24] Choudhury, M.; Nath, S.S. and Nath, R.K., ZnO: PVP Quantum dot Ethanol sensor, *Journal of sensor Technology*, Issue1, pp 86-90, 2011.
- [25] Nath, S.S.; Choudhury, M. and Nath, R.K., Syntheses of PVP embedded ZnO quantum dots and the investigation of their methanol sensing properties, *J. Nanotechnology Progress International*, Issue 4, 2011.
- [26] Nath, S.S.; Choudhury, M.; Nath, R.K. and Gope, G., PVA embedded ZnO quantum dots for methanol sensing, *Nanotrends- A journal of nanotechnology and its application*, vol 8, Issue 3, p 1, 2010.
- [27] Choudhury, M.; Nath, S.S.; Nath, R.K.; Chakder, D.; Gope, G. and Das, R., ZnO quantum dots in SBR latex for methanol sensing, *Assam University journal of Sc. and Tech.*, vol.6, No 2, pp 46-50, 2010.
- [28] Nath, S.S.; Choudhury, M.; Nath, R.K. and Gope, G., Acetone sensing property of ZnO quantum dots embedded on PVP, *Sensors and actuators B: Chemical*, vol. 148, pp 353-357, 2010.

- [29] Choudhury, M.; Nath, S.S.; Nath, R.K.; Gope, G. and Chakder, D., Acetone Sensing of ZnO quantum dots embedded in PVA matrix, *Advanced Science Letter.*, vol. No. 1, p. 6, 2010.